Critical number in scattering and escaping problems in classical mechanics

Salvador Addas-Zanata* and Clodoaldo Grotta-Ragazzo†
Instituto de Matemática e Estatística, Universidade de São Paulo, R. do Matão 1010, CEP 05508-900, São Paulo-SP, Brazil
(Received 17 January 2001; revised manuscript received 16 July 2001; published 24 September 2001)

Scattering and escaping problems for Hamiltonian systems with two degrees of freedom of the type kinetic plus potential energy arise in many applications. Under some discrete symmetry assumptions, it is shown that important quantities in these problems are determined by a relation between two canonical invariant numbers that can be explicitly computed.

DOI: 10.1103/PhysRevE.64.046216 PACS number(s): 05.45.−a

I. INTRODUCTION

Invariant tori are very important in the global dynamics of two degree of freedom Hamiltonian systems. They split the phase space in unconnected components. For several physically relevant systems, the existence of such invariant tori, and therefore the understanding of the phase-space structure, can only be achieved through numerical investigation. In this paper, an analytic criterion for the existence of certain families of invariant tori is presented. These families are important in some problems of escaping from and scattering off a potential well.

The class of systems such that our results apply can be described as follows. The Hamiltonian function is of the type kinetic plus potential energy,

$$H=\tfrac{1}{2}(p_x^2+p_y^2)+V(x,y), \tag{1}$$

where V has two critical points: a minimum P_m and a saddle-point P_s. The energy of the saddle point, which will be called critical energy and will be denoted E_{cr}, is $V(P_s)=E_{\mathrm{cr}}$. For energy values below E_{cr} the corresponding energy-level sets have two distinct components, one bounded and one unbounded. The bounded component projects to the configuration space (x,y) inside what will be called the potential well (see Fig. 1 for a topological representation of the level curves of V). For $H=E_{\mathrm{cr}}$, these two components touch at the equilibrium corresponding to P_s and for $H>E_{\mathrm{cr}}$, the two components merge into a single unbounded component. Notice that E_{cr} plays an important role in the dynamics. For energy values below E_{cr}, there is always a large quantity (in a measure sense) of bounded orbits trapped inside the potential well, while for energy values above E_{cr}, this may not occur.

An important example that belongs to the above class is the Hamiltonian system for the motion of a charged particle in the field of a magnetic dipole (see, for instance [1]), also called the Stormer system. Due to the rotation symmetry of the magnetic field, this system can be reduced to two degrees of freedom. For a given value of angular momentum and in convenient time and length scales, its Hamiltonian function is

$$H=\frac{1}{2}(p_x^2+p_y^2)+V(x,y),\quad V(x,y)=\frac{1}{2}\left(\frac{1}{x}-\frac{x}{(x^2+y^2)^{3/2}}\right)^2, \tag{2}$$

where x is the radial coordinate and y is the coordinate along the dipole axis. It is well known that V satisfies the above properties, so the level curves of the Stormer potential V are topologically as in Fig. 1: V has two critical points, a minimum P_m and a saddle-point P_s, such that $V(P_s)=E_{\mathrm{cr}}=1/32$ and for energy values below E_{cr}, the corresponding energy-level sets have two distinct components, one bounded and one unbounded. For $H=E_{\mathrm{cr}}$, these two components touch at the equilibrium corresponding to P_s and for $H>E_{\mathrm{cr}}$, the two components merge into a single unbounded component.

In this paper, two different problems will be considered for systems similar to the Stormer system, contained in the class defined below expression (1). The first is the so-called ‘‘escaping problem’’ or ‘‘escaping from a potential well,’’ that is: for a given distribution of initial conditions inside the potential well with fixed energy $E>E_{\mathrm{cr}}$ to determine the amount of solutions that remain inside the potential well after time $t>0$. This type of escaping problem had been re-

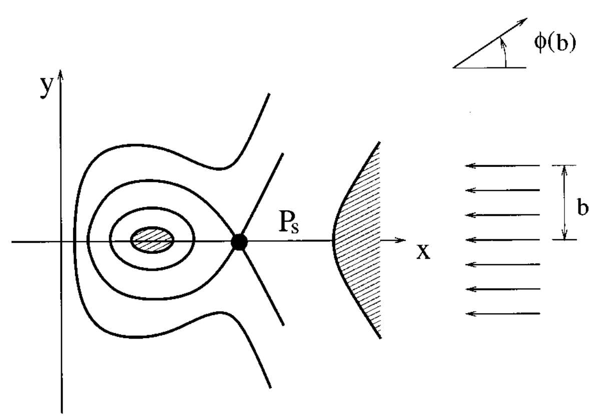

FIG. 1. Topological representation of the level sets of a typical potential function for the class we are considering. The shaded region corresponds to an energy level set below the energy of the saddle point P_s.

*Current address: Department of Mathematics, Princeton University, Fine Hall-Washington Road, Princeton, NJ 08544-1000. Email address: szanata@math.princeton.edu

†Email address: ragazzo@ime.usp.br

cently considered by Contopoulus *et al.* [2] and Kandrup *et al.* [3] in a series of papers that were the main motivation for the present paper. Escaping problems appear in several branches of physics and chemistry (see, for instance, [3,4] and references therein). The second problem addressed in this paper is the so-called ''scattering problem.'' For instance, consider the Stormer system and a family of initial conditions parametrized by an ''impact-parameter'' b with constant energy $E>E_{\rm cr}$, see Fig. 1. Most of these initial conditions will be scattered off the potential well and will become asymptotically free as t tends to infinity. These scattered solutions can be characterized by their asymptotic angle $\phi(b)$ as shown in Fig. 1. In this case, the scattering problem consists in determining the angle $\phi(b)$ as a function of the impact-parameter b. The scattering problem for other systems (or even for this one) can be defined in terms of other input-output variables instead of $b\rightarrow\phi(b)$. Scattering problems have been extensively studied, in particular in the context of chaotic systems. The reader can find many references on the subject in the special volume, Chaos 3, issue 4 (1993) (in particular, see [5] for a review) and also [6]. The scattering problem for the Stormer system has been considered, for instance, in [7].

From a theoretical point of view, escaping and scattering problems are better understood for systems that either are integrable or have fully hyperbolic recurrent sets. The systems considered here are mostly in between these two extreme cases. In the context of the Stormer system, our main result for the escaping problem can be summarized in the following way. For E larger than but close to $E_{\rm cr}$ solutions initially in the potential well can escape to infinity. This certainly happens for solutions on the x axis with initial velocity parallel to it. Nevertheless, escape may not occur for most solutions, if there exists a torus that projects to the configuration space like the one shown in Fig. 4(a). This torus blocks the ''exit'' from the potential well for ''most'' solutions. To be more precise about what we mean by ''most solutions,'' it is necessary to consider the limit $E\rightarrow E_{\rm cr}$ and to introduce the concept of a family of blocking tori. A *family of blocking tori is a set of invariant tori, one torus T_E for each $E\in(E_{\rm cr},\bar{E})$, for some $\bar{E}>E_{\rm cr}$ sufficiently close to $E_{\rm cr}$, such that each T_E splits the phase space into one bounded component and one unbounded component and such that T_E tends to a curve C* as $E\rightarrow E_{\rm cr}$. *Each torus T_E is called a blocking torus*. By $T_E\rightarrow C$ as $E\rightarrow E_{\rm cr}$ we mean convergence with respect to the Hausdorff metric, namely,

$$\max\{\mathrm{dist}(z,C):\ z\in T_E\}+\max\{\mathrm{dist}(z,T_E):\ z\in C\}\rightarrow 0$$
$$\text{as}\ \ E\rightarrow E_{\rm cr}.$$

The main result in this paper is to give a computable criterion for the existence of blocking tori in a class of systems that include the Stormer system. The implications of the existence of blocking tori for scattering problems is the following. A blocking torus restrict the access of all incoming solutions to a small phase-space region inside the potential well. Since most of the recurrent dynamics happens inside the potential well and recurrence is the main source of singularities in scattering functions, one expects that the regularity of these functions may strongly depend on the existence or not of a family of blocking tori.

Our criterion for the existence of blocking tori is a consequence of some previous mathematical and numerical investigations on systems with ''saddle-center loops'' [8–11]. Part of this work is presented in Sec. II. In Sec. III the results presented in Sec. II are applied to the Stormer systems and to three other systems that were studied in [3,2,12]. Section IV is a conclusion where we point out the main ideas in this paper.

II. THE CRITICAL NUMBER

In order to simplify the presentation, this section is divided in several subsections.

A. Hypotheses and the saddle-center loop map

Although the results described here are valid for a wider class of systems (see references below) in this section, we only consider Hamiltonian systems with two degrees of freedom of the form kinetic plus potential energy:

$$H=\tfrac{1}{2}[p_1^2+p_2^2]+U(q_1,q_2), \qquad (3)$$

where,

(a) U is analytic,

(b) $U(q_1,q_2)=\tfrac{1}{2}[-\nu^2q_1^2+\omega^2q_2^2]+\mathcal{O}((q_1^2+q_2^2)^{3/2})$, with $\omega>0,\nu>0$,

(c) $\partial_{q2}U(q_1,0)=0$, for any value of q_1,

(d) equation $U(q_1,0)=0$ has a nontrivial nondegenerated solution q_{1c} and no solutions in $(0,q_{1c})$.

The potential of the Stormer system (2) satisfies these hypotheses with $q_1=x$, $q_2=y$, and with $(q_1,q_2)=(0,0)$ replaced by P_s. The above systems have two important properties

(1) the origin is an equilibrium point of saddle-center type, namely, it is associated to a pair of real $\pm\nu$ and a pair of imaginary $\pm i\omega$ eigenvalues,

(2) the phase-space plane $\{q_1,p_1,q_2=p_2=0\}$ is invariant and it contains an orbit Γ homoclinic to the origin $p_1=p_2=q_1=q_2=0$.

The invariant set given by the saddle-center equilibrium and the homoclinic orbit Γ will be called *saddle-center loop*. From a topological point of view, a saddle-center loop is similar to a periodic orbit (of ''infinite period'') in phase space. Moreover, for system (3), the saddle-center loop is placed exactly where one can expect a possible family of blocking tori to accumulate (think about the Stormer system). These facts suggest two things: first, one can use Poincaré sections to study the saddle-center loop and second, families of blocking tori may be related to invariant circles

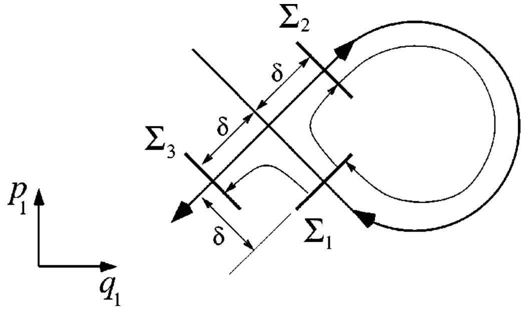

FIG. 2. Diagram showing the Poincaré sections Σ_1, Σ_2, and Σ_3 used to define mappings L and G.

on the induced Poincaré map. However, some difficulties appear when one tries to define a Poincaré map for a saddle-center loop due to the presence of the unstable equilibrium in the loop. In order to overcome this difficulty, a Poincaré map for the saddle-center loop will be defined by the composition of two distinct maps: one related to the passage of solutions near the saddle-center equilibrium denoted by L and another related to the traveling of solutions near Γ denoted by G. In order to define these mappings, it is first necessary to study the dynamics near the saddle-center equilibrium. The quadratic part of H is given by

$$H_L=\tfrac{1}{2}[p_1^2+p_2^2]+\tfrac{1}{2}[-\nu^2 q_1^2+\omega^2 q_2^2]. \tag{4}$$

This implies that the origin has a one-dimensional stable manifold W^s, a one-dimensional unstable manifold W^u, and a two-dimensional center manifold W^c. Within the linear approximation, these manifolds are given by $W^s=\{p_1=-\nu q_1, p_2=q_2=0\}$, $W^u=\{p_1=\nu q_1, p_2=q_2=0\}$, $W^c=\{p_1=q_1=0, p_2, q_2\}$. The part of W^s with $q_1>0$ $(q_1<0)$ will be denoted as W^s_+ (W^s_-) and the part of W^u with $q_1>0$ $(q_1<0)$ will be denoted as W^u_+ (W^u_-). Notice that Γ coincides either with W^s_+ and W^u_+ or with W^s_- and W^u_- (this follows from a simple analysis in the invariant $\{q_1,p_1\}$ plane). To simplify the presentation, it is assumed that Γ coincides with W^s_+ and W^u_+. Now, let Σ_1, Σ_2, and Σ_3 be three planar Poincaré sections (three-dimensional) transversal to W^s_+, W^u_+, and W^u_-, respectively, as shown in Fig. 2. Sections Σ_1, Σ_2, and Σ_3, are locally parametrized by q_2, p_2, and E, where E is again the energy. In order to simplify the computations, it is convenient to define canonical variables Q_1,P_1,Q_2,P_2

$$q_1=(P_1+Q_1)\frac{1}{\sqrt{2\nu}},\quad p_1=(P_1-Q_1)\frac{\sqrt{\nu}}{\sqrt{2}},$$

$$q_2=(P_2+Q_2)\frac{1}{\sqrt{2\omega}},\quad p_2=(P_2-Q_2)\frac{\sqrt{\omega}}{\sqrt{2}},$$

in such a way that H_L becomes

$$H_L=-\nu P_1 Q_1+\omega I,$$

$$\text{where}\quad I=\tfrac{1}{2}[\omega^{-1}p_2^2+\omega q_2^2]=\tfrac{1}{2}[P_2^2+Q_2^2].$$

Using these coordinates and the approximation H_L to H, one can parametrize Σ_1 as

$$Q_1=\delta=\text{const}>0,\quad P_1=\frac{\omega I-E}{\nu\delta}.$$

Similarly, one gets explicit expressions for Σ_2 and Σ_3. The integration of the linearized vector field near the origin gives the linear flow

$$\begin{pmatrix} Q_1(t)\\ P_1(t)\\ Q_2(t)\\ P_2(t)\end{pmatrix}=\begin{pmatrix} e^{-\nu t} & 0 & 0 & 0\\ 0 & e^{+\nu t} & 0 & 0\\ 0 & 0 & \cos(\omega t) & \sin(\omega t)\\ 0 & 0 & -\sin(\omega t) & \cos(\omega t)\end{pmatrix}\times\begin{pmatrix} Q_1(0)\\ P_1(0)\\ Q_2(0)\\ P_2(0)\end{pmatrix}. \tag{5}$$

This flow induces a discontinuous Poincaré map L: $\Sigma_1\to\Sigma_2\cup\Sigma_3$ given by the following relations (see Fig. 2).

(i) If $(Q_2,P_2,E)\in\Sigma_1$ is such that $\omega I>E$ (namely, $P_1>0$) then $L(Q_2,P_2,E)=(Q_2',P_2',E')\in\Sigma_2$ is given by [Z and Z' denote the column vectors (Q_2,P_2) and (Q_2',P_2'), respectively,]

$$E'=E,\quad Z'=R(\theta)Z,$$

where $R(\theta)$ is the rotation matrix of angle θ

$$R(\theta)=\begin{pmatrix}\cos\theta & -\sin\theta\\ \sin\theta & \cos\theta\end{pmatrix} \tag{6}$$

and $\theta=\theta(I,E)$ is given by

$$\theta(I,E)=-\frac{\omega}{\nu}\ln\left(\frac{\delta}{P_1}\right)=\frac{\omega}{\nu}\ln(\omega I-E)-\frac{\omega}{\nu}\ln(\delta^2\nu).$$

(ii) If $(Q_2,P_2,E)\in\Sigma_1$ is such that $\omega I<E$ (namely, $E>0$ and $P_1<0$) then $L(Q_2,P_2,E)=(Q_2',P_2',E')\in\Sigma_3$ is given by the same expressions as in item (i)

$$E'=E,\ \ Z'=R(\theta)Z,$$

except that θ is given by

$$\theta(I,E)=-\frac{\omega}{\nu}\ln\left(\frac{-\delta}{P_1}\right)=\frac{\omega}{\nu}\ln(E-\omega I)-\frac{\omega}{\nu}\ln(\delta^2\nu).$$

(iii) If $(Q_2,P_2,E)\in\Sigma_1$ is such that $\omega I=E$ (namely, $E\geqslant 0$ and $P_1=0$) then the solution that leaves Σ_1 is in the stable manifold of either a periodic orbit in W^c $(E>0)$ or the saddle-center equilibrium $(E=0)$. So the flow does not define the Poincaré map. In this case, $L(Q_2,P_2,E)=(Q_2',P_2',E')$ is defined to be in Σ_2 with coordinates given by $(Q_2',P_2',E')=(Q_2,P_2,E)$.

A Poincaré map G: $\Sigma_2 \to \Sigma_1$ is defined in the usual way by the flow near Γ. If $(Q_2,P_2,E)\in\Sigma_2$ then $G(Q_2,P_2,E) = (Q_2',P_2',E')\in\Sigma_1$ is given by

$$E=E', \quad Z'=C(\delta)Z+Eu(\delta)+\mathcal{O}(E^2+\|Z\|^2), \tag{7}$$

where $C(\delta)$ is a two-by-two matrix [the (Q_2,P_2) components of the derivative of G with respect to (Q_2,P_2) at $(Q_2,P_2,E)=(0,0,0)$] and $u(\delta)$ is a vector [the (Q_2,P_2) components of the derivative of G with respect to E at $(Q_2,P_2,E)=(0,0,0)$]. The invariance of the plane $\{q_1,p_1,q_2=0,p_2=0\}$ by the flow implies that $G(0,0,E) = (0,0,E)$ and therefore in this case $u(\delta)=0$. The flow expression (5) implies that if $\delta=\delta_0+D$ varies, where δ_0 is some fixed positive number, then $C(\delta)$ changes as $C(\delta_0+\Delta)=R(K')C(\delta_0)R(K')$ where $K'\in(0,2\pi]$ can assume any value depending on Δ. Writing $C(\delta_0)=A_0R(K_0)$ where A_0 is symmetric [polar decomposition of $C(\delta_0)$] and choosing Δ conveniently, one concludes that $C(\delta)$ can be written as $C(\delta)=AR(K)$ where A is a diagonal matrix. Using the simplectic property of the flow, one gets that the determinant of A is one. Therefore, the expression for the (Q_2,P_2) components of G, denoted as $\hat{G}$, within the linear approximation and with a convenient choice of δ is given by

$$Z'=\hat{G}(Z)=AR(K)Z, \text{ where } A=\begin{pmatrix} \alpha & 0 \\ 0 & 1/\alpha \end{pmatrix}, \quad \alpha\geqslant 1. \tag{8}$$

Let Σ_{1E} and Σ_{2E} be the restrictions of Σ_1 and Σ_2, respectively, to the energy level set $H=E$, for E close to zero. Since the dynamics preserves energy, it is convenient to restrict maps L and G to Σ_{1E} and Σ_{2E}, respectively. The above expressions for L imply that the (Q_2,P_2) components of L, denoted by $\hat{L}$, restricted to Σ_{1E} are given by

$$Z'=\hat{L}(Z,E)=R(\theta)Z,$$

$$\text{where } \theta(I,E)=\gamma \ln\|I-\omega^{-1}E\|+K', \tag{9}$$

where $\gamma=\omega/\nu$, $K'\in[0,2\pi)$ is some fixed number that depends on δ, and Z' belongs to either Σ_{2E} or Σ_{3E} depending on $\omega I-E\geqslant 0$ or $\omega I-E<0$, respectively (if $\omega I+E$ then $Z'=Z$). Notice that for $E=0$, $\hat{L}$: $\Sigma_{10}\to\Sigma_{20}$, $\hat{G}$: $\Sigma_{20}\to\Sigma_{10}$, and the composition $F=G\circ L$: $\Sigma_{10}\to\Sigma_{10}$ is well-defined. In this case, $Z'=F(Z)=AR(2\gamma\ln\|Z\|-\gamma\ln 2+K'+K)Z$ and with a simple rescaling $Z\to\beta Z$, $Z'\to\beta Z'$, where $2\gamma\ln\beta=\gamma\ln 2-K-K'$, one can write F in the simple form

$$Z'=F(Z)=AR(2\gamma\ln\|Z\|)Z, \tag{10}$$

that will be called *saddle-center loop map*. Several approximations were made in the derivation of F. In particular, the linearized flow was used to describe the dynamics near the equilibrium. So, $\delta>0$ must be chosen small. It can be shown [9,10] that the real Poincaré map from $\Sigma_{10}\to\Sigma_{10}$ differs from the one above by a term bounded by $K\|Z\|^2$, where K is some positive constant.

The results presented in this section are due to several authors, especially Lerman [13] and Mielke, Holmes, and O'Reilly [14]. The normal form theorem used to study the integrable nonlinear dynamics near the saddle-center loop is due to Moser [15] with a supplement of Rüssmann [16] (see also [17], Appendix 8). Some early ideas related to the dynamics in systems with saddle-center equilibria using Moser's theorem can be found in Conley [18,19], Churchill, Pecelli, and Rod [12] and Churchhill and Rod [20] (see, also earlier work by the same authors cited in these references), and Llibre, Martinez, and Simó [21]. Mappings G, L, and the saddle-center loop map F as presented here are due to Lerman [13] and Mielke, Holmes, and O'Reilly [14], independently.

B. The invariants α and γ

The dynamics of the saddle-center loop map depends on the two parameters γ and α. The parameter $\gamma=\omega/\nu$ is the ratio between the modulus of two eigenvalues ω and ν and therefore is invariant under any change of coordinates (it is invariant even under time reparametrization). The parameter α is harder to compute and is related to the flow linearized at the orbit Γ. Let $\overline{q_1}(t)$ be the q_1 component of $\Gamma(t)$. The (q_2,p_2) components of the vector field linearized at Γ are

$$\dot{q}_2=p_2,$$
$$\dot{p}_2=-[\omega^2+S\{\overline{q_1}(t)\}]q_2, \tag{11}$$

where

$$\omega^2+S(q_1)=\omega^2+\mathcal{O}(q_1)=\partial_{q_2,q_2}V(q_1,0).$$

In the variables (Q_2,P_2) these equations become

$$\dot{Q}_2=\omega P_2,$$

$$\dot{P}_2=-[\omega+\omega^{-1}S\{\overline{q_1}(t)\}]Q_2. \tag{12}$$

For a given $\delta>0$, let $t_-(\delta)$ and $t_+(\delta)$ be two time values such that the (Q_1,P_1) coordinates of $\Gamma[t_-(\delta)]$ are $(0,\delta)$ and the (Q_1,P_1) coordinates of $\Gamma[t_+(\delta)]$ are $(\delta,0)$. Let $\psi(t_-,t)$ be a fundamental system of solutions of Eq. (12) such that $\psi(t_-,t_-)$ is the identity matrix. Then, matrix $C(\delta)$ appearing in Eq. (7) is given by $\psi(t_-,t_+)$ and $\alpha(\delta)$ is the square root of the largest eigenvalue of $C(\delta)C(\delta)^\dagger$, where $C(\delta)^\dagger$ denotes the transpose of $C(\delta)$ [geometrically, $\alpha(\delta)$ is the largest semiaxis of an ellipsis that is the image of a unit circle by $C(\delta)$]. In principle, the value of $\alpha(\delta)$ depends not only on δ but also on the coordinates used near the saddle-center equilibrium. However, a computation using Moser coordinates [or assuming as true the linear flow approximation (5)] shows that $\alpha(\delta)$ does not depend on δ. Still, this property depends on this special system of coordinates. In order to present a characterization of α that does not depend on a special coordinate system, one defines $\delta=\delta_0$ and $\delta_n=\delta_0 e^{-2\pi n/\gamma}$. Then, one takes the limit as $n\to\infty$ to get: $\delta_n\to 0$, $t_\pm\to\pm\infty$, and $\psi(t_-,t_+)\to\psi(-\infty,+\infty)$: $TW^c\to TW^c$, where TW^c is the tangent manifold to W^c at the origin (this limit is explained in detail in [8], Theorem 3). The trace of $\psi(-\infty, +\infty)$ does not depend on coordinate systems anymore, but depends on the choice of δ_0. Nevertheless, one can prove (as in [8], Theorems 3 and 4) that the maximum of the trace of $\psi(-\infty, +\infty)$ for δ_0 varying in the interval $[\delta e^{-2\pi/\gamma},\gamma]$ is equal to $\alpha+\alpha^{-1}$ and it does not depend either on δ or on the coordinate system. This construction gives an invariant definition for α. In order to compute α, it is necessary to take a special limit $\psi(-\infty, +\infty)$ of the fundamental solution of Eq. (12). For the particular systems in this paper, this limit gets a very familiar form. Notice that both equations (11) and (12) are equivalent to second-order differential equations for q_2 and Q_2, respectively. Moreover, both equations for q_2 and Q_2 are the same and are given by

$$\ddot{q}_2=-[\omega^2+S\{\overline{q_1}(t)\}]q_2, \tag{13}$$

where $S[\overline{q_1}(t)]$ decays exponentially fast to zero as $t\to\pm\infty$. Equation (13) is a one-dimensional Schrödinger equation similar to those appearing in one-dimensional quantum scattering problems. It has a complex-valued solution ϕ with the following asymptotic behavior:

$$\phi(t)\to\hat{A}e^{i\omega t}+Be^{-i\omega t}\quad\text{as}\quad t\to-\infty,$$

$$\phi(t)\to e^{i\omega t}\quad\text{as}\quad t\to\infty,\quad \hat{A},B\quad\text{complex.} \tag{14}$$

$\hat{A}$ and B are the usual scattering coefficients of quantum mechanics. In [8] (Theorem 4) it is shown that the maximum with respect to δ_0 of the trace of the limit $\psi(-\infty, +\infty)$ (as discussed above), which is equal to $\alpha+\alpha^{-1}$, is also equal to $2\sqrt{|B|^2+1}$. Therefore, one gets that $\alpha\geqslant 1$ is given by

$$\alpha=|B|+\sqrt{|B|^2+1}, \tag{15}$$

where $|B|$ is determined by the one-dimensional scattering problem (13)–(14).

The number α can be also understood in a different and more geometric way. The center manifold of the saddle-center equilibrium is foliated by periodic orbits ζ_E, one for each energy $E>0$. In the linear flow approximation (5) ζ_E is a circle of radius $\sqrt{2E/\omega}$ in the plane $\{Q_1=P_1=0,Q_1,P_2\}$. The stable (unstable) manifold of ζ_E is a cylinder that intersects Σ_{1E} (Σ_{2E}) at a circle C_{1E} (C_{2E}) with the same radius. The global mapping G maps $C_{2E}\in\Sigma_{2E}$ to a closed curve $C'_{1E}\in\Sigma_{1E}$ that is approximately an ellipsis if $E>0$ is small. In general, C'_{1E} intersects the circle C_{1E} transversally. Let β' denote the area outside C_{1E} and inside C'_{1E} and let β be the area inside C_{1E}. Since G restricted to Σ_{2E} preserves area, then $0\leqslant\beta'/\beta<1$. Let β_* be the limit of $\beta'(E)/\beta(E)$ as $E\to 0$. Then one gets

$$\cos\left(\beta_*\frac{\pi}{2}\right)=\frac{2}{\alpha+\alpha^{-1}}. \tag{16}$$

Notice that if the unstable and stable manifolds of ζ_E coincide then $\alpha=1$. This is a necessary condition for integrability obtained in [13] and [14]. Notice that in terms of the scattering coefficient B, a necessary condition for integrability is $B=0$, namely, a resonance in the "quantum scattering problem" (13)–(14). The number α first appeared in [13] and [14]. An invariant characterization of it was given in [8] that was the source for most of the presentation above.

C. A class of examples where α can be easily computed

In general, it is not easy to solve the scattering equation (13). In most cases this can only be done numerically. Nevertheless, there is an important class of potentials where this problem can be solved analytically [8]. This class is described in the following. Suppose that the potential V in Eq. (3) satisfies the following additional hypotheses:

$$V(q_1,0)=-\tfrac{1}{2}\nu^2q_1^2+\frac{\delta}{n+1}q_1^{n+1},$$

$$\partial_{q2,q2}V(q_1,0)=\omega^2+\beta q_1^{n-1}. \tag{17}$$

This implies that the solution homoclinic to the origin satisfies $q_2=p_2=0$ and

$$\ddot{q}_1=+\nu^2q_1-\delta q_1^n.$$

It can be checked that the q_1 component of Γ is given by

$$q_1(t)=C\,\mathrm{sech}^{2/(n-1)}\left(\frac{t\nu(n-1)}{2}\right),$$

$$\text{where}\quad C=\left(\frac{(n+1)\nu^2}{2\delta}\right)^{1/(n-1)}.$$

This implies that Eq. (13) becomes

$$\ddot{q}_2=-\left[\omega^2+\frac{\beta(n+1)\nu^2}{2\delta}\mathrm{sech}^2\left(\frac{t\nu(n-1)}{2}\right)\right]q_2. \tag{18}$$

This is a well-known one-dimensional Schrödinger equation problem that can be solved using hyper geometric functions. The modulus of B is given in [22], Sec. 25, Eq. 4, as

$$|B|^2=\frac{\cos^2[(\pi/2)\sqrt{\eta}]}{\sinh^2(\pi\epsilon)},\quad\text{if}\quad\eta>0,$$

$$|B|^2=\frac{\cosh^2[(\pi/2)\sqrt{-\eta}]}{\sinh^2(\pi\epsilon)},\quad\text{if}\quad\eta<0, \tag{19}$$

where

$$\epsilon=\frac{2\omega}{(n-1)\nu},\qquad\eta=\frac{\beta}{\delta}\frac{8(n+1)}{(n-1)^2}+1.$$

Then, α follows from these expressions and from $\alpha=|B|+\sqrt{|B|^2+1}$ [Eq. (15)].

D. Families of blocking tori and the critical number

In the introduction, a family of blocking tori was defined using the topology of the energy-level sets of the Stormer system as a model. That definition can be easily generalized to systems that satisfy the hypotheses of Sec. II A. In this case, a blocking torus splits the phase space into two connected components but none of them has to be necessarily bounded. For these systems, the existence of a family of blocking tori accumulating at Γ is implied by the existence of a family of invariant curves accumulating at the trivial fixed point of the saddle-center map F, Eq. (10). Before explaining this claim, it is necessary to study the dynamics of F. The following two paragraphs were essentially taken from [11].

Map F has among other symmetries a remarkable one: it is invariant under discrete dilation $Z \to e^{\pi/\gamma}Z$ [namely, $F(e^{\pi/\gamma}Z) = e^{\pi/\gamma}F(Z)$]. In particular, this symmetry implies that the fixed point $Z=(0,0)=\underline{0}$ is stable when α is sufficiently close to $\alpha=1$. In fact, for $\alpha=1$, F leaves all circles centered at $\underline{0}$ invariant (F is just a rotation in each circle). Far from the origin, F is analytic and the KAM (Kolmogorov, Arnold, and Moser) theorem can be used to prove that, if $|\alpha-1|$ is sufficiently small, then invariant closed curves surrounding $\underline{0}$ exist. Since there is one such a curve there are infinitely many, due to the dilation symmetry, and these curves accumulate at $\underline{0}$ (where F is not differentiable).

The dilation symmetry also suggests a beautiful mechanism for the instability of $\underline{0}$ when α is large. For $\alpha>1$, if F has a fixed point p distinct from $\underline{0}$, then it has an infinite family of fixed points given by $e^{k\pi/\gamma}p$, $k\in\mathbb{Z}$. Indeed, an explicit computation shows that F has four families of fixed points. The first family is denoted by z_k, $k\in\mathbb{Z}$, where $z_k = e^{\pi k/\gamma}z_0$. The elements of the second family are given by $-z_k$. The element z_0 has coordinates

$$P_2 = \exp\left(\frac{\delta}{\gamma} - \frac{\pi}{4\gamma}\right)\cos\delta, \quad Q_2 = \exp\left(\frac{\delta}{\gamma} - \frac{\pi}{4\gamma}\right)\sin\delta,$$

where $\delta = \arctan(1/\alpha) \in (0,\pi/4)$. The linearization of F around z_k and $-z_k$, for all k, is associated to the same pair of eigenvalues (λ,λ^{-1}), determined by $\lambda+\lambda^{-1} = 2+2\gamma(\alpha-\alpha^{-1})$. This implies that all $\pm z_k$ are hyperbolic. Now, suppose the unstable manifold of z_0 intersects transversally the stable manifold of z_1. Then, the dilation symmetry of F implies that the unstable manifold of z_k intersects transversally the stable manifold of z_{k+1} for all $k\in\mathbb{Z}$. The same is valid for the family $-z_k$, $k\in\mathbb{Z}$. So, due to the discrete symmetry, the existence of a transversal heteroclinic orbit connecting z_0 to z_1 implies the existence of two infinite heteroclinic chains, or ''Arnold's transition chains'' [24], which implies (besides a lot of ''chaos'') the instability of $\underline{0}$. In order to show that this scenario indeed occurs, it is still necessary to show that the unstable manifold of z_0 intersects the stable manifold of z_1 transversally. This is related to the nonexistence of homotopically nontrivial invariant curves in the saddle-center loop map. It was proved in [10] that the above transition chain exists if $\gamma(\alpha-\alpha^{-1})>1$. For the real saddle-center loop map, that takes into account the higher-order corrections to F, it was proved [10] the existence of a semi-infinite heteroclinic chain connecting points arbitrarily close to the saddle-center loop to points at finite distance of it.

In [11], a numerical study of F was done in order to estimate the region in the parameter space $\gamma>0$, $\alpha\geqslant 1$, where invariant circles surrounding $\underline{0}$ exists. Very curiously the following simple criterion was obtained.

Stability criterion. Let c be the number (stability number):

$$c = \gamma(\alpha - \alpha^{-1}). \tag{20}$$

There is a critical value of c, denoted as c_c and called critical number, such that

• If $c<c_c$, then there are invariant circles surrounding $\underline{0}$, so all orbits of F are bounded and $\underline{0}$ is a stable fixed point.
• If $c>c_c$ then there are no invariant circles surrounding $\underline{0}$ and F has an infinite heteroclinic chain connecting $\underline{0}$ to infinity.

An approximated value of c_c, probably overestimated, is $c_c = 1/\sqrt{2}$.

Remark: The above criterion was obtained numerically. Both the form of the critical curve and the critical number $c_c = 1/\sqrt{2}$ are only approximations. The computation near the breakup of the last invariant curve is delicate. For instance, for some particular values of γ, it was numerically verified a stability-instability transition at $c_c = 0.55$ [23].

Notice that the appearance of the above heteroclinic chain reminds us of (and it is very similar to) the so-called ''resonance overlap criterion'' of Chirikov [24]. This idea of resonances overlap when applied to the standard map also produces infinite heteroclinic chains. A remarkable property of the saddle-center loop map F is that this infinite heteroclinic chain of F implies a semi-infinite heteroclinic chain for the original Hamiltonian system (3) [10].

Now, we turn back to the question of the existence of families of blocking tori. All the discussion above supposes the energy E to be zero. Nevertheless, the concept of families of blocking tori requires the existence of invariant tori for $E>0$. In fact, using the KAM theorem (as, for instance, in [10]) it can be shown that the existence of sufficiently smooth invariant circles surrounding $\underline{0}$ for $E=0$ imply the existence of perturbed invariant circles for $E\neq 0, |E|$ small. The statement is as follows. If the above invariant circles for $E=0$ exist, then given an $\epsilon>0$ there exists $\delta>0$ such that for $|E|<\delta$ the mapping $G\circ L$ restricted to Σ_{1E} has an invariant circle with a radius less than ϵ. This conclusion clearly implies the existence of a family of blocking tori associated to the saddle-center equilibrium at the origin of system (3). So, the stability criterion above can also be used as a criterion for the existence of families of blocking tori. More information about invariant curves for $E>0$ can be found in [10] (in particular, in Fig. 4 of [10] one can find a diagram that motivated the definition of a family of blocking tori).

E. The saddle-center scattering map

In Sec. II A we presented maps L and G to describe the dynamics near a saddle-center loop of a system satisfying certain hypotheses. In this section, the dynamics generated by these maps will be studied for a fixed small value of $E>0$. For simplicity, the index E will be omitted from Σ_{1E},

Σ_{2E}, and Σ_{3E}, and the restriction of the (Q_2,P_2) components of L and G to the energy-level set E will be denoted also by L and G, respectively. So, the dynamics near the saddle-center loop in this case is determined by the pair of mappings [see Eqs. (9) and (8)]

$$L:\ \Sigma_1\to\Sigma_2\cup\Sigma_3,$$

$$Z'=L(Z)=R(\gamma\ln|\|Z\|^2-2\omega^{-1}E|+K')Z,$$

and

$$G:\ \Sigma_2\to\Sigma_1,\quad Z'=G(Z)=AR(K),$$

where K and K' are two constant phases in $(0,2\pi)$ and the image of L is in Σ_2 if $\|Z\|^2-2\omega^{-1}E\geqslant 0$ otherwise it is in Σ_3 (see Fig. 2). For a system satisfying the hypotheses of Sec. II A, a typical scattering problem, similar to the one for the Stormer system mentioned in the introduction and illustrated in Fig. 1, is the following. The incoming particles are given by a line of initial conditions with fixed energy $E>0$ at $q_1=0$ with $p_1=\dot{q}_1=v>0$, v constant satisfying $0<v<\sqrt{2E}$. For E small, from the linearized Hamiltonian H_L (4), one gets that this set of initial conditions corresponds to a circle in phase space given by

$$Q_1=-\frac{v}{\sqrt{2\nu}},\quad P_1=\frac{v}{\sqrt{2\nu}},\quad Q_2^2+P_2^2=\frac{2}{\omega}\left(E-\frac{v^2}{2}\right).$$

The linearized flow (5) maps this circle to another circle S in Σ_2 with the same radius. So one can consider $S\in\Sigma_2$ as the input of the scattering process. It is clear that if the only exit from the potential well is over the saddle-center equilibrium at the origin, then any scattered solution must hit Σ_3. Therefore, a suitable output for the scattering problem is the (Q_2,P_2) components (or any function of them) of the intersection of an exiting solution with Σ_3.

Under some circumstances, as discussed below, the scattering problem presented above is approximately determined by the dynamics of L and G in the following way. The initial condition for the scattering process is given by the circle $S\in\Sigma_2$. This circle is mapped by G to an ellipsis $G(S)\in\Sigma_1$, see Fig. 3. The points in $G(S)$ have two possible ways. If they are outside the circle $\|Z\|^2=2\omega^{-1}E$ (represented by a dotted circle in Fig. 3) then they are mapped back to Σ_2 by L. If they are inside this circle, then they are mapped to Σ_3 by L. The scattering process for the points in Σ_3 is finished and the corresponding output value are their (Q_2,P_2) components. Moreover, the scattering time in this case may be taken as one, because they were scattered after one cycle of iteration of G and L. Then the points $L\circ G(S)\in\Sigma_2$ are mapped again to Σ_2 and so on, see Fig. 3. The result is that from this iteration scheme (which we call ''saddle-center scattering map'') one can get all scattering functions.

The procedure described in the above paragraph approximates well the real scattering process under two circumstances. At first, $E>0$ has to be sufficiently small. At second, the stability number c of the previous section must be less than the critical one $c_c\approx 1/\sqrt{2}$, namely, the system must have a family of blocking tori. If this last condition is not verified, then points initially close to $Z=(Q_2,P_2)=(0,0)$ can escape to infinity under iterations of $L\circ G$. Therefore, they will never hit Σ_3. Moreover, mappings G and L approximate the real dynamics only when $\|Z\|$ is not large. Even when c is large, the scattering results obtained with mappings G and L may be a good approximation to the real scattering in its first few iterates.

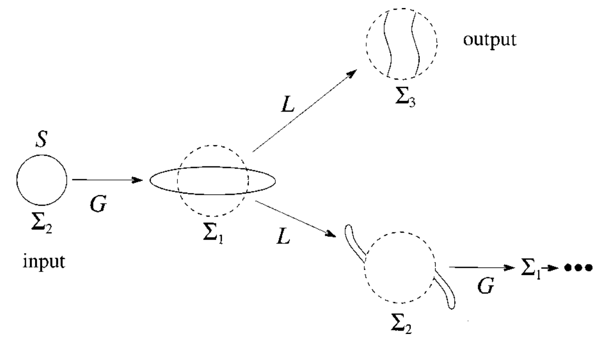

FIG. 3. Diagram showing the sequence of mappings used to define the saddle-center scattering map. Notice that points outside the dotted circle in Σ_1 are mapped to Σ_2 and then mapped back to Σ_1 by G. Those points inside the dotted circle in Σ_2 are mapped outside the potential well to Σ_3. For them the scattering process is over.

We point out that the scattering map defined in [25], which consists of reinjecting the scattered solutions, may be easily obtained in the context of the saddle-center scattering map. This is done through the identification of Σ_3 and Σ_2. The result is a mapping from $\hat{F}$: $\Sigma_1\to\Sigma_1$ given by

$$Z'=\hat{F}(Z)=AR(\gamma\ln|\|Z\|^2-2\omega^{-1}E|+K'+K)Z,$$

where K and K' are constants in $[0,2\pi)$ and the mapping is the identity if $\|Z\|^2-2\omega^{-1}E=0$.

III. APPLICATIONS

The goal in this section is to apply the results presented in the previous one to four examples. The first three are taken from [3,2,12].

A. Example 1

In this example, the Hamiltonian function is

$$H=\tfrac{1}{2}(p_x^2+p_y^2)+V(x,y),$$

$$V(x,y)=\tfrac{1}{2}(x^2+y^2)-\tfrac{1}{3}y^3+\mu x^2 y.$$

This is Eq. (3) of [3]. For $\mu=1$, it is the well-studied Hénon-Heiles system [26,12]. For any value of $\mu\geqslant 0$, the potential function has a saddle point at $(x,y)=(0,1)$ with an associated critical energy $E_{\mathrm{cr}}=1/6$. With the change of variables $y=1-q_1$, $x=q_2$, one gets

$$V(x,y)=\tfrac{1}{2}\,[-q_t^2+(1+2\mu)q_2^2]+\tfrac{1}{3}\,q_1^3-\mu q_1 q_2^2.$$

This system satisfies the hypotheses in Sec. II C with: $\nu=1$, $n=2$, $\delta=1$, $\omega=\sqrt{1+2\mu}$, $\beta=-2\mu$. So, $\epsilon=2\sqrt{1+2\mu}$, $\eta=-48\mu+1$, and the values of $|B|$ follow from Eq. (19). For instance, for $\mu=0$, $\mu=0.43$, $\mu=0.49$, and $\mu=1$, one obtains $|B|=0$, $|B|\approx 0.25$, and $|B|\approx 0.89$, respectively. Using Eq. (15), the stability number can be written in terms of $|B|$ as

$$c=2\gamma|B|,$$

which implies $c=0$, $c\approx 0.55$, $c\approx 1/\sqrt{2}$, and $c\approx 3.1$, for $\mu=0$, $\mu=0.43$, $\mu=0.49$, and $\mu=1$, respectively. In this case, the criterion for the nonexistence of invariant tori around the saddle-center loop using the critical number $c_c=1/\sqrt{2}$ gives for μ the critical value $\mu=0.49$. A more careful numerical analysis of the dynamics of the saddle-center loop map F for the particular parameter values of this problem showed, however, that the breaking up of the last invariant tori of F happens for $\mu=0.43$ that corresponds to a $c_c=0.55$ [23]. This is in agreement with numerical simulations of the real flow [23]. So, in this example, the critical value of μ is taken as 0.43.

It is interesting to visualize projections of blocking tori in the configuration space. Consider the sequence of Figs. 4 for different parameter values μ and for a fixed value of energy equal to 0.17 (above $E_{\mathrm{cr}}=1/6$). In Figs. 4(a) ($\mu=0$) and 4(b) ($\mu=0.4$), we show projections of invariant tori on the configuration space that block the escaping channel over the saddle-center equilibrium. In Fig. 4c ($\mu=0.7$) we exhibit a single solution starting near the boundary of the potential well that escapes from it. This shows that there is no variant torus near the saddle-center loop blocking the exit of the potential well.

In order to illustrate the dependence of a scattering problem for this system on the parameter μ, consider a scattering function ψ defined in the following way. For a given $E>0$, let $\{x=b,\ y=1.1,\ p_x=0,\ p_y<0\}$ be a one parameter family of input initial conditions where p_y is determined by $H=E=\mathrm{const}$ and the impact-parameter b is defined in a maximal interval where $V(b,1.1)\leqslant E$. Consider the solution generated by the initial condition associated to b and suppose that for some time $T(b)$ this solution hits the phase-space hypersurface $\{y=1\}$ with $p_y>0$ and $x=\psi(b)$. The functions $b\to T(b)$ and $b\to\psi(b)$ will be called as time delay and scattering return map, respectively. It seems from a sequence of graphs of the scattering return map, obtained through the variation of μ for $E=0.17$ fixed, that near $\mu=0.43$ the rate (with respect to μ) of loss of regularity of $b\to\psi(b)$ is enhanced. Nevertheless, the transition that occurs near $\mu=0.43$ can be much easily seen through a plot of an averaged time delay function $\overline{T}(\mu)$ as shown in Fig. 5. This function $\overline{T}$ is obtained taking the average of $T(b)$ over many equally spaced values of b for a fixed value of μ.

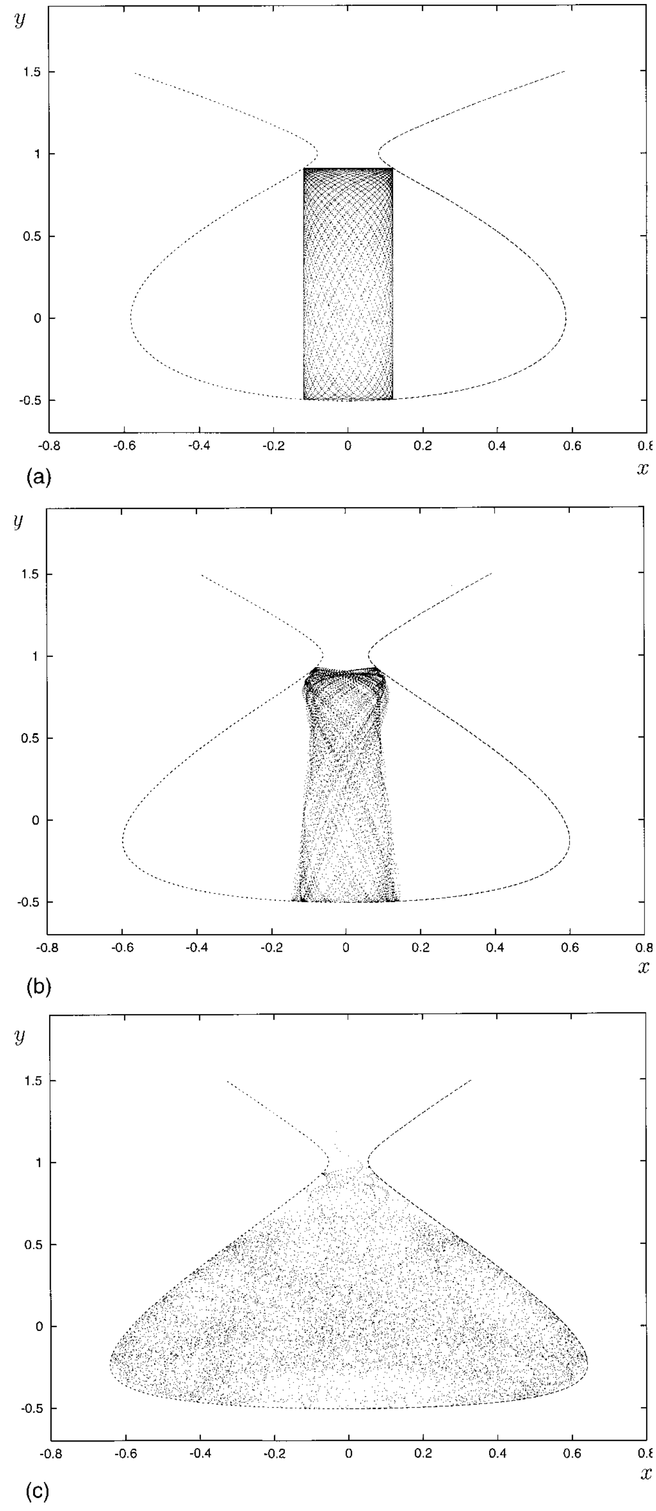

FIG. 4. Projections on the configuration space of orbits of the Hénon-Heiles family with energy equal to 0.17 and initial conditions $y(0)=0$, $p_x(0)=0$, $p_y(0)>0$, and: (a) for $\mu=0$, $x(0)=0.12$; (b) for $\mu=0.4$, $x(0)=0.12$; (c) for $\mu=0.7$, $x(0)=0.58$.

The potential V above has two more saddle points $x=\pm(1/2\mu\sqrt{\mu})\sqrt{1+2\mu}=\pm\overline{x}$, $y=-1/(2\mu)=\overline{y}$, at energy $E=(1+3\mu)/(24\mu^3)$. There is a homoclinic solution to each saddle-center equilibrium corresponding to each of these

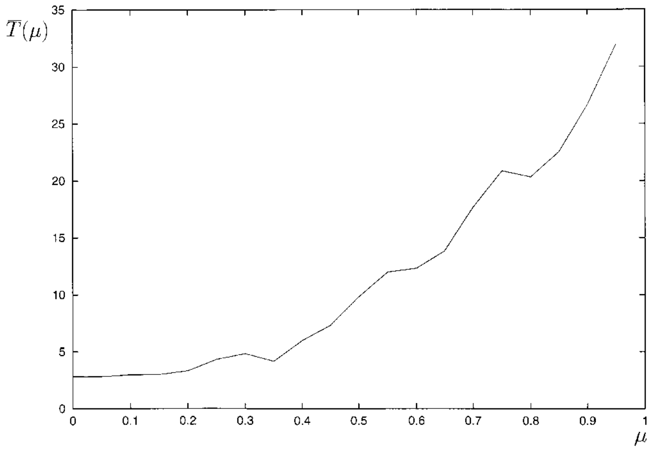

FIG. 5. Graph of the averaged time delay function $\overline{T}(\mu)$.

saddle points. These homoclinic solutions are given by $x(t) = \pm\bar{x}u(t)$, $y(t)=\bar{y}u(t)$, where u satisfies $\ddot{u}=-u+u^2$, $u(t)\to 1$ as $t\to\pm\infty$. As above, the coefficients γ and $|B|$ can be computed explicitly. For $\mu=1$, the potential is symmetric with respect to rotations of $2\pi/3$ radians, which implies that γ and $|B|$ are the same for the three homoclinic saddle-center loops. These saddle-center loops are related to an escaping problem that will be discussed after the next two examples.

B. Example 2

In this example, the Hamiltonian function is

$$H=\tfrac{1}{2}(p_x^2+p_y^2)+V(x,y), \quad V(x,y)=\tfrac{1}{2}(x^2+y^2)-xy^2.$$

This is Eq. (8.1) of [12] and after some rescaling of coordinates and time, this is Eq. (2) of [3]. The potential V has a pair of saddle points $(x,y)=(1/2)(1\pm\sqrt{2})$ at energy 1/8. The saddle-center equilibria related to these saddle points have eigenvalues ± 1 and $\pm i\sqrt{2}$. There is one homoclinic solution to each saddle-center equilibrium. Introducing coordinates

$$x=\frac{1}{\sqrt{3}}(\hat{q}_1-\sqrt{2}q_2), \quad y=\frac{1}{\sqrt{3}}(\sqrt{2}\hat{q}_1+q_2), \quad \hat{q}_1=\frac{\sqrt{3}}{2}-q_1,$$

one gets a system satisfying the hypotheses in Sec. II C. The same reasoning as in the previous example gives: $\nu=1$, $\omega=\sqrt{2}$, $\gamma=\sqrt{2}$, $|B|\approx 0.259$, $c=2\gamma|B|\approx 0.807>\sqrt{2}$. This implies that there are no families of blocking tori accumulating at the saddle-center loops.

C. Example 3

In this example, the Hamiltonian function is

$$H=\tfrac{1}{2}(p_x^2+p_y^2)+V(x,y), \quad V(x,y)=\tfrac{1}{2}(x^2+y^2)-\tfrac{1}{2}x^2y^2.$$

This is Eq. (8.2) of [12] and after some rescaling of coordinates and time, this is Eq. (1) of [3]. The potential V has four saddle-points $(x,y)=(\pm 1,\pm 1)$ at energy 1/2. The saddle-center equilibria related to these saddle points have eigenvalues $\pm\sqrt{2}$ and $\pm i\sqrt{2}(\gamma=1)$. There is one pair of heteroclinic orbits connecting the equilibria at $(x,y)=(1,1)$ and $(x,y)=(-1,-1)$, and one pair of heteroclinic orbits connecting the equilibria at $(x,y)=(1,-1)$ and $(x,y)=(-1,1)$. In principle, the results in Sec. II A, for homoclinic orbits to saddle-center equilibria do not apply. Nevertheless, there is a simple adaptation [9,10] of the above-presented results to the case of heteroclinic loops. Again, the scattering problem for the determination of α is explicitly solvable and gives: $|B|\approx 0.119$, $c=2\gamma|B|\approx 0.238<1/\sqrt{2}$. This implies that there are invariant tori accumulating at the saddle-center heteroclinic loop, and therefore, a family of blocking tori for $E>E_{\rm cr}$, $E\to E_{\rm cr}$.

D. The escaping problem and the dynamics for examples 1, 2, and 3

The escaping problem for the systems in Examples 1, 2, and 3 was studied by Kandrup *et al.* [3]. They have a parameter ϵ in their systems that coincides with the parameter μ in Example 1 and that in Examples 2 and 3, after some rescaling, can be identified with the energy (in fact, what they do is to fix an energy and vary this parameter; after the rescaling, this is equivalent to fix the parameter and vary the energy). So, below, the reader can think of ϵ as if it were the energy. In particular, their ϵ_0 is equivalent to the energy $E_{\rm cr}$ of the saddle-center equilibrium. In their own words, one of their main conclusions was: (the following paragraph was taken from the abstract of [3]):

''For ϵ below a critical value ϵ_0, escapes are impossible energetically. For somewhat higher values, escape is allowed energetically but still many orbits never escape. The escape probability P computed for an arbitrary orbit ensemble decays toward zero exponentially. At or near a critical value $\epsilon_1>\epsilon_0$ there is a rather abrupt qualitative change in the behavior. Above $\epsilon_1,\ldots,$. The transitional behavior observed near ϵ_1 is attributed to the breakdown of some specially significant KAM tori or cantori... .''

In principle, it is not easy to relate the results in [3] to those in here. They studied the escaping problem for a range of energies that include values far from the energy $E_{\rm cr}$ of the saddle-center equilibrium, while here, all results concern energies near $E_{\rm cr}$. However, there is an interesting fact in their results that makes it possible to establish a connection between their critical ϵ_1 and the concept of a family of blocking tori introduced here. For Examples 2 and 3 above, the value of $E_{\rm cr}$ is 0.125 and 0.5, respectively, and the values of ϵ_1 they found are equivalent to energies $E=0.165^{+0.006}_{-0.014}$ and $E_1=1.176\pm 0.0024$, respectively. For Example 1, they fixed the energy of the initial conditions $E=0.167$, which implies that escape is energetically possible for $\mu>\mu_0=1$, and found a critical value of μ_1 (or ϵ_1) of 1.1 ± 0.5. Under these circumstances, the saddle-center loops that are relevant for the escaping problem are those presented at the end of Sec. III A. Their energy is $E_{\rm cr}=0.135^{+0.015}_{-0.013}$ depending on $\mu_1=1.1\pm 0.5$. Since $\mu_1\approx 1$, these saddle-center loops have numbers γ and $|B|$ ''close to'' those computed for the saddle-center loop on the x axis for $\mu=1$. Therefore they are unstable. Notice that in Examples 1 and 2, there is no family of blocking tori accumulating on those saddle-center loops that are relevant for the escaping problem. In both cases, Kandrup *et al.* found a "critical energy E_1" close to the energy $E_{\rm cr}$ of the saddle-center loops. In Example 3, there are families of blocking tori accumulating on the heteroclinic saddle-center loops and Kandrup *et al.* found a value of E_1 more than twice as large as $E_{\rm cr}$. So, our conclusion is that systems with unstable saddle-center loops, and therefore with no family of blocking tori, may have a value of E_1 (equivalent to the critical ϵ_1 of Kandrup *et al.*) "close" to $E_{\rm cr}$ while those systems having families of blocking tori may have a value of E_1 "far" from $E_{\rm cr}$. It is not easy to give a more quantitative meaning for this last statement. The question is complex and even the definition of E_1 that is based on numerical investigation is not quantitatively clear and sharp.

The dynamics of the mappings in Examples 1, 2, and 3 for E near $E_{\rm cr}$ is also related to the parameters α and γ. For Example 1, this idea was discussed in [23]. It is well known [26] that for $\mu=1$, the dynamics of the system in Example 1 is mostly stochastic inside each energy level set $E<E_{\rm cr}$ for E near $E_{\rm cr}$. In this case, the saddle-center loop is unstable (there is no family of invariant tori accumulating on it). On the other hand, it was reported in [26] that the system of example 3 has no observable large scale stochasticity for $E<E_{\rm cr}$ and E near $E_{\rm cr}$. In this case the saddle-center loop is stable and there are invariant tori accumulating on it. This indicates that the stability or instability of the saddle-center loop is related to the existence or not, respectively, of large stochastic regions at energy-level sets E close to $E_{\rm cr}$.

E. The Stormer system

The Stormer system (2) also has a saddle-center loop contained in the plane $\{x,p_x,y=p_y=0\}$. The scattering problem associated to it (13)–(14) cannot be solved analytically as above but can be solved numerically. In this case, one finds the saddle-center loop parameters $\omega^2=3/64$, $\nu^2=1/32$, $\gamma=\sqrt{3/2}$ and $\alpha\approx5.8$, which implies that there are no invariant tori around the saddle-center loop. This seems to be in agreement with the scattering results in [7], which shows a predominance of hyperbolicity and with other numerical results on the chaotic dynamics of the Stormer problem (see, for instance, [1]).

IV. CONCLUSION

In this paper, the concept of a family of blocking tori is introduced. For systems satisfying the hypotheses in Sec. II A a family of blocking tori is a set of invariant tori, one for each energy $E>E_{\rm cr}$, such that the limit of the set as $E\to E_{\rm cr}$ is a saddle-center loop. In Sec. II we presented a criterion for the existence of families of blocking tori that uses two invariant numbers γ and α related to the saddle-center loop. These numbers can be computed in several interesting examples, as for instance, those presented in Sec. III.

In Sec. II E we presented a pair of "universal" mappings G and L depending on the parameters α and γ that may describe the scattering off a potential well near the critical energy $E_{\rm cr}$ provided the system has a family of blocking tori. It would be interesting to numerically check the energy range of validity of this claim.

The mechanism for breaking up families of blocking tori discussed here consists in the creation of an infinite heteroclinic chain [10,11]. The critical parameter for this chain creation may be related to some tangencies between invariant manifolds of different hyperbolic periodic orbits. Tangencies between invariant manifolds were found by Lai *et al.* [27] as a mechanism for "chaotic scattering enhancement" that they called "crisis in chaotic scattering."

ACKNOWLEDGMENTS

C.G.R. is partially supported by CNPq (Brazil) Grant No. 301817/96-0. S.A.Z. was supported by FAPESP (Brazil) Grant No. 96/08981-3, and is under support by CNPq Grant No. 200564/00-5.

[1] A. J. Dragt and J. M. Finn, J. Geophys. Res. **81**, 2327 (1976).
[2] G. Contopoulus, H. E. Kandrup, and D. E. Kaufmann, Physica D **64**, 310 (1993); C. V. Siopis, G. Contopoulus, and H. E. Kandrup, Ann. N.Y. Acad. Sci. **751**, 205 (1995); C. V. Siopis, G. Contopoulus, H. E. Kandrup, and R. Dvorak, *ibid.* **773**, 221 (1995).
[3] H. E. Kandrup, C. Siopis, G. Contopoulus, and R. Dvorak, Chaos **9**, 381 (1999).
[4] A. M. Ozorio de Almeida, N. de Leon, M. A. Mehta, and C. C. Marston, Physica D **46**, 265 (1990).
[5] E. Ott and T. Tel, Chaos **3**, 417 (1993).
[6] B. Ruckerl and C. Jung, J. Appl. Phys. **27**, 55 (1994); C. Jung and T. H. Seligman, Phys. Rep. **285**, 78 (1997); C. Jung, C. Lipp, and T. H. Seligman, Ann. Phys. (Leipzig) **275**, 151 (1998); T. Butikofer, C. Jung, and T. H. Seligman, Phys. Lett. A **265**, 76 (2000).
[7] C. Jung and H.-J. Scholz, J. Phys. A **21**, 2301 (1988); B. Ruckerl and C. Jung, *ibid.* **27**, 6741 (1994).
[8] C. Grotta Ragazzo, Commun. Math. Phys. **166**, 255 (1994).
[9] C. Grotta Ragazzo, Commun. Pure Appl. Math. **50**, 105 (1997).
[10] C. Grotta Ragazzo, Commun. Math. Phys. **184**, 251 (1997).
[11] C. Grotta Ragazzo, Phys. Lett. A **230**, 183 (1997).
[12] P. C. Churchill, G. Pecelli, and D. L. Rod, Springer Lecture Notes in Physics, Vol. 93 (Springer, Berlin, 1979), p. 76.
[13] L. M. Lerman, Sel. Math. Sov. **10**, 297 (1991).
[14] A. Mielke, P. Holmes, and O. O'Reilly, J. Dyn. Diff. Eqns. **4**, 95 (1992).
[15] J. Moser, Commun. Pure Appl. Math. **11**, 257 (1958).
[16] H. Rüssmann, Math. Ann. **154**, 285 (1964).
[17] J. Henrard, Dynam. Report: Exp. Dyn. Syst. **2**, 117 (1993), Springer, Berlin.
[18] C. Conley, SIAM (Soc. Ind. Appl. Math.) J. Appl. Math. **16**, 732 (1968).
[19] C. Conley, J. Diff. Eqns. **5**, 136 (1969).
[20] R. C. Churchill and D. L. Rod, J. Diff. Eqns. **37**, 351 (1980).

[21] J. Llibre, R. Martinez, and C. Simó C., J. Diff. Eqns. **58**, 104 (1985).
[22] L. D. Landau and E. M. Lifshitz, *Quantum Mechanics, Nonrelativistic Theory* (Pergamon, Oxford, 1965).
[23] J. C. Bastos de Figueiredo, C. Grotta Ragazzo, and C. P. Malta, Phys. Lett. A **241**, 35 (1998).
[24] B. V. Chirikov, Phys. Rep. **52**, 264 (1979).
[25] C. Jung, J. Phys. A **19**, 1345 (1986); **20**, 719 (1987).
[26] M. Hénon and C. Heiles, Astron. J. **69**, 73 (1964).
[27] Y-C. Lai, C. Grebogi, R. Blumel, and I. Kan, Phys. Rev. Lett. **71**, 2212 (1993).